ISME

An Analytical Shear Factor for FGM Circular Plates with Non-uniform Elastic Foundations and Normal and Shear Tractions

M. Shariyat[†]
Associate Professor

M.M. Alipour*
Ph.D

The available shear correction factors have mainly been developed for homogeneous isotropic plates and/or assuming that no shear tractions are imposed on the top and bottom surfaces of the plate. In the present research, a more general case of a circular functionally graded plate subjected to non-uniform normal and shear tractions at the top and bottom surfaces is considered. These non-uniform tractions may stem from the imposed non-uniform inclined tractions at the top surface and resting on the non-uniform Winkler-Pasternak elastic foundations. Instead of using the approximate numerical methods, the solutions are derived using a pure analytical method. In this regard, influences of the proposed analytical correction factor are evaluated on results of both the modal and the stress analyses.

Keywords: shear correction factor, circular functionally graded plate, non-uniform tractions, vibration, stress, non-uniform elastic foundation.

1 Introduction

Circular disks or plates are among the main engineering components that may be employed in both static and dynamic systems, due to e.g., their axisymmetric configuration, minimum perimeter, simplest manufacturing technologies and costs, and simplest fitting requirements (into another components or supports). On the other hand, in many practical applications, due to differences in the design requirements of the top and bottom surfaces of the pale, it is necessary to use different material properties for the top and bottom surfaces of the plate. In these circumstances, it is advantageous to use functionally graded materials for the plate, to prevent any discontinuities in the transverse distributions of the material properties and stresses.

For thin and relatively thin plates, using the higher-order plate theories does not lead to pronounced enhancements in comparison to the first-order ones. Some researchers have proven that in these cases, results of the higher-order and even the elasticity theories may

[†] Corresponding author, Associate Professor, Faculty of Mechanical Engineering, K.N. Toosi University of Technology, Pardis Street, MolaSadra Avenue, Vanak Square, Tehran, Iran, m_shariyat@yahoo.com shariyat@kntu.ac.ir

[*] Ph.D, Faculty of Mechanical Engineering, K.N. Toosi University of Technology, Pardis Street, MolaSadra Avenue, Vanak Square, Tehran, Iran

exhibit more inaccuracies [1], in some situations. For this reason, many researchers have used the first-order plate theories, employing adequate shear correction factors to modify the computed strain energy of the transverse shear stresses [2-5].

The available shear correction factors have mainly been proposed for special transverse distributions of the material properties, tractions types, loading conditions, and boundary conditions [6]. Mindlin [7] derived two different shear coefficients: one was dependent on Poisson's ratio and the other was a constant. Stephen [8] by matching between the long flexural wavelength phase velocity predictions of the second mode of Mindlin finite plate theory and the exact Rayleigh-Lamb frequency equation came to a conclusion that the best correction factor is due to Mindlin (that includes the Poisson ratio effect). Andrew [9] derived a shear correction coefficient for a plate with an infinite spatial extent. Liu and Soh [10] proposed two methods for determination of the shear correction factor and proposed the *0.8* shear correction factor for the homogeneous elastic materials. Kirakosyan [11] introduced an extended concept of two correction coefficients for an orthotropic plate subjected to tangential shears at the top and bottom surfaces using the energy equivalence principle. Two shear correction expressions that account for the influence of the transverse normal stress component were derived by Batista [12] where the first was a slightly modified Mindlin factor. Sometimes, the shear correction factor concept may be used to impose the continuity condition of the transverse stresses at the layer interfaces [13]. The traditional correction factors have mainly been derived on the basis of situations where distribution of the transverse shear stress is parabolic. In functionally graded plates, this assumption may not hold, as the material properties distribution is generally non-uniform and non-linear.

In the above mentioned researches, material properties were assumed to be constant within each layer. To extend Mindlin's correction factor to the FGM plates, Efraim and Eisenberger [14] replaced Poisson's ratio with the average Poisson ratio of the mixture. Extending an approach previously used for the composite beams, Nguyen et al. [15] proposed shear correction factors for the FGM plates using the equivalent shear energy method.

The forgoing brief review reveals that the available shear correction factors have mainly been developed based on either assuming homogeneous isotropic material properties or assuming that no shear tractions are imposed on the top and bottom surfaces of the plate. In the present research, a more general case of a circular functionally graded plate subjected to simultaneous non-uniform normal and shear tractions at the top and bottom surfaces is considered, due to presence of the non-uniform inclined traction at the top surface and a non-uniform Winkler-Pasternak elastic foundation at the bottom surface of the plate. Instead of using the approximate numerical methods, the solutions are derived using a pure analytical method. The employed analytical method is the differential transform method (DTM) that is a semi-analytical technique that uses Taylor's series expansion. Employing the DTM enables obtaining highly convergent and accurate results and analytical solutions for the differential or integro-differential equations [16-18]. By using this method, the governing differential equations can be reduced to recurrence relations and the boundary conditions may be transformed into a set of algebraic equations. In the present paper, influences of using the derived analytical correction factor on results of both the modal and the stress analyses are evaluated.

2 Governing equations of motion of the circular functionally graded plate

Consider an FGM circular plate that is resting on a non-uniform two-parameter elastic foundation and undergoing non-uniform normal and shear tractions, as shown in Figure (1).

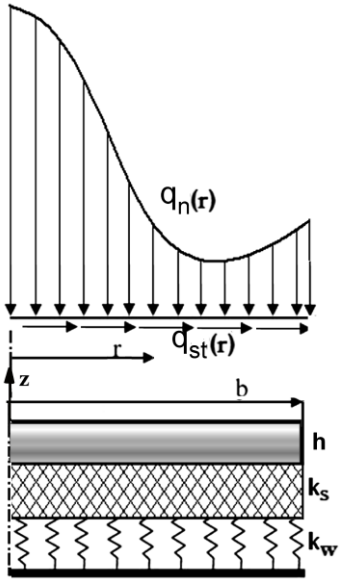

Figure 1 Parameters of the functionally graded circular plate and the elastic foundation, as well as the adopted coordinate system.

Based on the Mindlin first-order shear-deformation plate theory for small deflections, the displacement field may be described as follows:

$$\begin{aligned} u(r,z,t) &= u_0(r,t) + z\psi_r(r,t) \\ w(r,z,t) &= w_0(r,t) \end{aligned} \tag{1}$$

where u and w are the radial and transverse displacement components of an arbitrary point of the thickness and u_0, w_0, and ψ_r are, respectively, the radial and transverse displacements of the reference layer (e.g., the mid-layer) and rotation of the radial section. The coordinate z is measured from the reference layer and is positive upward. Therefore, the strain components may be expressed as:

$$\begin{aligned} &\varepsilon_r = u_{,r} = u_{0,r} + z\psi_{r,r}, \quad \varepsilon_\theta = \frac{u}{r} = \frac{u_0 + z\psi_r}{r}, \\ &\varepsilon_z = w_{,z} = 0, \qquad \gamma_{rz} = u_{,z} + w_{,r} = \psi_r + w_{,r} \end{aligned} \tag{2}$$

where the comma symbol stands for the partial derivative.
Therefore, if the functionally graded plate is constructed from linear elastic constituent materials, the stress components may be derived from:

$$\begin{aligned} \sigma_r &= \frac{E}{1-\nu^2}(\varepsilon_r + \nu\varepsilon_\theta) = \frac{E}{1-\nu^2}\left[\left(u_{0,r} + \nu\frac{u_0}{r}\right) + z\left(\psi_{r,r} + \nu\frac{\psi_r}{r}\right)\right], \\ \sigma_\theta &= \frac{E}{1-\nu^2}(\varepsilon_\theta + \nu\varepsilon_r) = \frac{E}{1-\nu^2}\left[\left(\frac{u_0}{r} + \nu u_{0,r}\right) + z\left(\frac{\psi_r}{r} + \nu\psi_{r,r}\right)\right], \\ \sigma_z &= 0, \qquad \tau_{rz} = \frac{E}{2(1+\nu)}\gamma_{rz} = \frac{E}{2(1+\nu)}(\psi_r + w_{,r}) \end{aligned} \tag{3}$$

The governing equations are derived using Hamilton's equation:

$$\int_t (\delta K - \delta U + \delta V)dt = 0 \tag{4}$$

Where in increments of the strain energy (δU), kinetic energy (δK), and energy of the externally applied loads (δV) are:

$$\begin{aligned} \delta U &= \int_V \left\{ \sigma_r \delta(u_{0,r} + z\psi_{r,r}) + \sigma_\theta \delta\left(\frac{u_0 + z\psi_r}{r}\right) + \kappa\tau_{rz}\delta(\psi_r + w_{,r}) \right\} dV, \\ \delta K &= -\int_V \rho\{\ddot{u}\delta u + \ddot{w}\delta w\} dV, \\ \delta V &= \int_A \left[q_n \delta w + kw\delta w + k_s w_{,r}\delta w_{,r} + (q_{st} + q_{sb})\delta u_0 + \frac{h}{2}(q_{st} - q_{sb})\delta\psi_r \right] dA \end{aligned} \tag{5}$$

Here, κ is the so-called shear correction factor that is usually included in the first-order shear-deformation theories to correct the strain energy of the resulting transverse shear stresses. An accurate derivation procedure is proposed for this factor, in the next section. In Eq. (5), $q_n = q_0\left(1+\alpha_2 \mathrm{r}+\alpha_3 \mathrm{r}^2\right)$ and $k = k_w\left(1+\beta_2 r+\beta_3 r^2\right)$ are the non-uniformly distributed normal traction and Winkler coefficient of the elastic foundation, respectively, and q_{st} and q_{sb} are, respectively, the shear tractions of the top and bottom surfaces of the plate. k_s is the Pasternak coefficient of the elastic foundation and *b* is the outer radius of the plate [Figure (1)]. Integrals of Eq. (5) may be manipulated further through integration by parts, using the Green-Gauss rule to have:

$$\begin{aligned} \delta U &= \int_A \int_{-h/2}^{h/2} \left\{ -\left(\sigma_{r,r} + \frac{\sigma_r}{r}\right)\delta(u_0 + z\psi_r) + \frac{\sigma_\theta}{r}\delta(u_0 + z\psi_r) + \kappa\tau_{rz}\delta\psi_r - \kappa\left(\tau_{rz,r} + \frac{\tau_{rz}}{r}\right)\delta w \right\} dz\, dA \\ &\quad + \int_\Gamma \int_{-h/2}^{h/2} \{\sigma_r \delta(u_0 + z\psi_r) + \kappa\tau_{rz}\delta w\} r dz d\theta \\ \delta K &= -\int_A \int_{-h/2}^{h/2} \rho\left(\ddot{u}\delta u + \ddot{w}\delta w\right) dz\, dA \\ \delta V &= \int_A \left\{ q_0\left(1+\alpha_2 \mathrm{r}+\alpha_3 \mathrm{r}^2\right)\delta w + k_w\left(1+\beta_2 r+\beta_3 r^2\right) w\delta w - \frac{1}{r}(r k_s w_{,r})_{,r} + (q_{st} + q_{sb})\delta u_0 \right. \\ &\quad \left. + \frac{h}{2}(q_{st} - q_{sb})\delta\psi_r \right\} dA + \int_\Gamma k_s w_{,r}\, \delta w\, r d\theta \end{aligned} \tag{6}$$

where, Γ is the boundary of the plate. Substituting Eq. (6) into Eq. (4) leads to:

$$\begin{aligned} \int_t \int_A \int_{-h/2}^{h/2} \left\{ \left(\frac{\sigma_r - \sigma_\theta}{r} + \sigma_{r,r}\right)\delta(u_0 + z\psi_r) - \kappa\tau_{rz}\delta\psi_r + \left[\kappa\left(\tau_{rz,r} + \frac{\tau_{rz}}{r}\right) + q_0\left(1+\alpha_2 r+\alpha_3 r^2\right) \right] \right. \\ + k_w\left(1+\beta_2 r+\beta_3 r^2\right) \Big] \delta w + (q_{st} + q_{sb})\delta u_0 + \frac{h}{2}(q_{st} - q_{sb})\delta\psi_r \\ \left. - \rho\left(\ddot{u}_0 + z\ddot{\psi}_r\right)\delta(u_0 + z\psi_r) + \rho\ddot{w}\delta w \right\} dz\, dA\, dt = 0 \end{aligned} \tag{7}$$

Defining the following symbols for the transverse integrals of the stress and inertia quantities:

$$
\begin{aligned}
N_r &= \int_{-h/2}^{h/2} \sigma_r dz = A\left(u_{0,r} + \frac{\nu}{r}u_0\right) + B\left(\psi_{r,r} + \frac{\nu}{r}\psi_r\right) \\
N_\theta &= \int_{-h/2}^{h/2} \sigma_\theta dz = A\left(\frac{u_0}{r} + \nu u_{0,r}\right) + B\left(\frac{\psi_r}{r} + \nu\psi_{r,r}\right) \\
M_r &= \int_{-h/2}^{h/2} \sigma_r z dz = B\left(u_{0,r} + \frac{\nu}{r}u_0\right) + D\left(\psi_{r,r} + \frac{\nu}{r}\psi_r\right) \\
M_\theta &= \int_{-h/2}^{h/2} \sigma_\theta z dz = B\left(\frac{u_0}{r} + \nu u_{0,r}\right) + D\left(\frac{\psi_r}{r} + \nu\psi_{r,r}\right)
\end{aligned} \tag{8}
$$

$$
Q_r = \kappa \int_{-h/2}^{h/2} \tau_{rz} dz = \frac{(1-\nu)}{2}\tilde{A}(\psi_r + w_{,r}), \quad \tilde{A} = \kappa \int_{-h/2}^{h/2} \frac{E}{2(1+\nu)} dz
$$

$$
\begin{Bmatrix} A \\ B \\ D \end{Bmatrix} = \int_{-h/2}^{h/2} \frac{E}{1-\nu^2} \begin{Bmatrix} 1 \\ z \\ z^2 \end{Bmatrix} dz, \quad \begin{Bmatrix} I_0 \\ I_1 \\ I_2 \end{Bmatrix} = \int_{-h/2}^{h/2} \rho \begin{Bmatrix} 1 \\ z \\ z^2 \end{Bmatrix} dz
$$

Equation (7) may be rewritten as:

$$
\begin{aligned}
\int_t \int_A \Bigg\{ & \left(\frac{N_r - N_\theta}{r} + N_{r,r} - I_0\ddot{u}_0 - I_1\ddot{\psi}_r + q_{st} + q_{sb} \right)\delta u_0 \\
& + \left[\frac{M_r - M_\theta}{r} + M_{r,r} - Q_r + \frac{h}{2}(q_{st} - q_{sb}) - I_1\ddot{u}_0 - I_2\ddot{\psi}_r \right]\delta\psi_r \\
& + \left[Q_{r,r} + \frac{Q_r}{r} + q_0\left(1 + \alpha_2 r + \alpha_3 r^2\right) + k_w\left(1 + \beta_2 r + \beta_3 r^2\right)w - I_0\ddot{w} \right]\delta w \Bigg\} dA\, dt = 0
\end{aligned} \tag{9}
$$

Since Eq. (9) must hold for any arbitrary time interval, it may be concluded that the integrand of Eq. (9) has to be zero. On the other hand, since this conclusion must hold for any arbitrary values of the displacement increments, terms multiplied by these displacement increments should be zero:

$$
\begin{aligned}
\delta u_0 &: \quad \frac{N_r - N_\theta}{r} + N_{r,r} + q_{st} + q_{sb} = I_0\ddot{u}_0 + I_1\ddot{\psi}_r \\
\delta\psi_r &: \quad \frac{M_r - M_\theta}{r} + M_{r,r} - Q_{rz} + \frac{h}{2}(q_{st} - q_{sb}) = I_1\ddot{u}_0 + I_2\ddot{\psi}_r \\
\delta w &: \quad Q_{r,r} + \frac{Q_r}{r} + \frac{1}{r}(rN_r w_{,r})_{,r} + k_w\left(1 + \beta_2 r + \beta_3 r^2\right)w + q_0\left(1 + \alpha_2 r + \alpha_3 r^2\right) \\
& \quad - \frac{1}{r}(rk_s w_{,r})_{,r} = I_0\ddot{w}
\end{aligned} \tag{10}
$$

In the present research, distributions of the top and bottom shear tractions are also considered to be non-uniform, to obtain more general results:

$$
q_{st} = T_t\left(1 + \lambda_2 r + \lambda_3 r^2\right), \qquad q_{sb} = T_b\left(1 + \gamma_2 r + \gamma_3 r^2\right) \tag{11}
$$

Assuming that the FGM plate is fabricated from ceramic and metallic materials, variations of a representative material property P in the transverse direction may be assumed to be:

$$P = P_c V_c + P_m V_m \tag{12}$$

where, the subscripts *c* and *m* denote the ceramic and metal, respectively. Also, V_c and V_m , the volume fractions of the ceramic and metallic constituent materials, may be related to each other as follows:

$$V_c + V_m = 1 \tag{13}$$

The metal volume fraction is assumed to follow a power–law distribution [19]:

$$V_m = \left(\frac{1}{2} - \frac{z}{h}\right)^g \tag{14}$$

where *g* is the positive definite power–law index. From Eqs. (12-14), transverse variations of the modulus of elasticity, mass density, and Poisson's ratio of the resulting mixture may be obtained at an arbitrary point as:

$$\begin{aligned} E(z) &= (E_m - E_c)\left(\frac{z}{h} + \frac{1}{2}\right)^g + E_c \\ \rho(z) &= (\rho_m - \rho_c)\left(\frac{z}{h} + \frac{1}{2}\right)^g + \rho_c \\ \nu(z) &= (\nu_m - \nu_c)\left(\frac{z}{h} + \frac{1}{2}\right)^g + \nu_c \end{aligned} \tag{15}$$

Therefore, based on Eqs. (8,15):

$$\begin{aligned} A &= \int_{-h/2}^{h/2} \frac{E(z)}{1-\nu(z)^2} dz, \quad \tilde{A} = \kappa \int_{-h/2}^{h/2} \frac{E(z)}{2[1+\nu(z)]} dz \\ B &= \int_{-h/2}^{h/2} \frac{E(z)}{1-\nu(z)^2} z dz, \quad D = \int_{-h/2}^{h/2} \frac{E(z)}{1-\nu(z)^2} z^2 dz \end{aligned} \tag{16}$$

3 Distribution of the transverse shear stress according to the 3D elasticity theory

It is known that generally, the traditional approach of using the constitutive-based equations for determination of the through-thickness variations of the transverse shear stress does not lead to accurate results [20-24], especially when using the firs-order shear-deformation theory. In the present section, a general analytical shear correction factor is proposed for circular FGM plates subjected to non-uniform normal and shear tractions and resting on non-uniform Winkler-Pasternak elastic foundations.

Based on the three-dimensional theory of elasticity, the equations of motion of the axisymmetric circular plate in terms of the stress components may be expressed as:

$$\frac{\partial \sigma_r}{\partial r} + \frac{\sigma_r - \sigma_\theta}{r} + \frac{\partial \tau_{rz}}{\partial z} = \rho \ddot{u} \tag{17}$$

$$\frac{\partial \tau_{rz}}{\partial r} + \frac{\tau_{rz}}{r} + \frac{\partial \sigma_z}{\partial z} = \rho \ddot{w} \tag{18}$$

where σ_r, σ_θ, and σ_z are the normal and τ_{rz} is the shear stress components. Although the radial and transverse inertia body forces resulted from the ($\rho \ddot{u}$ and $\rho \ddot{w}$) term appeared in Eqs. (17,18) may affect the shear correction factor, their effects may be ignored in comparison to the transversely applied distributed tractions, especially for the thin plates. This assumption has been employed in derivation of all of the available shear correction factors. By

substituting the radial and circumferential stress from Eq. (3) into Eq. (17), the equilibrium equation in the radial direction necessitates that:

$$\frac{E(z)}{1-\nu(z)^2}\left(\bar{\nabla}^2 u_0 + z\bar{\nabla}^2\psi_r\right) + \frac{\partial\tau_{rz}}{\partial z} = 0, \quad \bar{\nabla}^2 \equiv \left(\frac{\partial^2}{\partial r^2} + \frac{1}{r}\frac{\partial}{\partial r} - \frac{1}{r^2}\right) \tag{19}$$

Integration of the elasticity equilibrium Eq. (19) across the plate thickness and using the following boundary condition,

$$\tau_{rz\left(z=-\frac{h}{2}\right)} = q_{sb} \tag{20}$$

one arrives at

$$\tau_{rz} = -F(z)\bar{\nabla}^2 u_0 - L(z)\bar{\nabla}^2\psi_r + q_{sb}, \tag{21}$$

where

$$\begin{Bmatrix} F(z) \\ L(z) \end{Bmatrix} = \int_{-\frac{h}{2}}^{z} \frac{E(z)}{1-\nu(z)^2}\begin{Bmatrix} 1 \\ z \end{Bmatrix} dz \tag{22}$$

By using the boundary condition of the top surface of the plate, $\nabla^2 u_0$ can be expressed in terms of the shear tractions of the top and bottom layers of the plate. Then, distribution of the transverse shear stress may be obtained based on Eq. (21) as

$$\tau_{rz\left(z=\frac{h}{2}\right)} = q_{st} \tag{23}$$

$$\tau_{rz} = \left(F(z)\frac{L_{\left(z=\frac{h}{2}\right)}}{F_{\left(z=\frac{h}{2}\right)}} - L(z)\right)\bar{\nabla}^2\psi_r + \left(1 - \frac{F(z)}{F_{\left(z=\frac{h}{2}\right)}}\right)q_{sb} + \frac{F(z)}{F_{\left(z=\frac{h}{2}\right)}}q_{st} \tag{24}$$

By integrating of the transverse shear stress (Eq. 24) across the plate thickness, the transverse shear force per unit length may be obtained as:

$$Q_r = \int_{-h/2}^{h/2}\left[\left(F(z)\frac{L_{\left(z=\frac{h}{2}\right)}}{F_{\left(z=\frac{h}{2}\right)}} - L(z)\right)\bar{\nabla}^2\psi_r + \left(1 - \frac{F(z)}{F_{\left(z=\frac{h}{2}\right)}}\right)q_{sb} + \frac{F(z)}{F_{\left(z=\frac{h}{2}\right)}}q_{st}\right]dz = X\bar{\nabla}^2\psi_r + Y \tag{25}$$

where

$$X = \int_{-h/2}^{h/2}\left(F(z)\frac{L_{\left(z=\frac{h}{2}\right)}}{F_{\left(z=\frac{h}{2}\right)}} - L(z)\right)dz, \quad Y = \int_{-h/2}^{h/2}\left[\left(1 - \frac{F(z)}{F_{\left(z=\frac{h}{2}\right)}}\right)q_{sb} + \frac{F(z)}{F_{\left(z=\frac{h}{2}\right)}}q_{st}\right]dz \tag{26}$$

Based on Eq. (25), $\bar{\nabla}^2\psi_r$ may be expressed in terms of Q_r. Substituting the resulting expression into Eq. (24), distribution of the transverse shear stress may be written as follows:

$$\tau_{rz} = \left(F(z)\frac{L_{\left(z=\frac{h}{2}\right)}}{F_{\left(z=\frac{h}{2}\right)}} - L(z)\right)\frac{Q_r - Y}{X} + \left(1 - \frac{F(z)}{F_{\left(z=\frac{h}{2}\right)}}\right)\tau_b + \frac{F(z)}{F_{\left(z=\frac{h}{2}\right)}}\tau_t \tag{27}$$

4 Derivation of the shear correction factor

The available shear correction factors have been derived for isotropic and homogeneous plate with shear tractions. Therefore, they are generally not suitable for heterogeneous functionally graded plates with shear tractions or elastic foundations that apply shear tractions (such as the present Winkler-Pasternak elastic foundation). Furthermore, since stiffness of the foundation of the plate varies in the radial direction, the governing equations of motion differ from those of the simple plates. The shear correction factor is determined in the present research base on equating of the shear strain energies of the transverse shear stress obtained based of the first-order plate theory and the three-dimensional theory of elasticity. Moreover, the available shear correction factors have mainly been derived based on the assumption of linear through-thickness distributions for the normal in-plane stresses. Due to transverse variations of the material properties across the thickness (e.g., according a power law), this assumption does not hold for structures with the transversely graded material properties. In the present research, the assumption of linear variations of the in-plane displacement component, that is a direct result of Eq. (1), is employed. However, this assumption leads to a linear through-thickness distribution for the in-plane stresses of the isotropic homogeneous plates.

Based on the first-order shear-deformation plate theory (FSDT), distribution of the transverse shear stress of the functionally graded plate may be determined from:

$$\tau'_{rz} = G(z)\left(\psi_r + w_{,r}\right) \tag{28}$$

By integrating Eq. (28) across the plate thickness, the relevant transverse shear force per unit length may be obtained as:

$$Q_r = \int_{-h/2}^{h/2} \tau'_{rz} dz = C\left(\psi_r + w_{,r}\right), \quad C = \int_{-h/2}^{h/2} G(z) dz \tag{29}$$

Comparing Eqs. (28,29) leads to the following result:

$$\tau'_{rz} = \frac{G(z)}{C} Q_r \tag{30}$$

The strain energy of the transverse shear stress may be calculated using Eq. (6). Substituting Eqs. (27) and (30) into the expression of the strain energy of the transverse shear stress, gives the following strain energy expressions that are associated with the three-dimensional theory of elasticity and the first-order shear-deformation plate theory, respectively:

$$\Pi_s = \frac{1}{2}\int_a^b \int_{-h/2}^{h/2} \frac{\tau_{rz}^2}{G(z)} dz dr = \frac{1}{2}\int_a^b \int_{-h/2}^{h/2} \frac{1}{G(z)} \left[\left(F(z) \frac{L_{\left(z=\frac{h}{2}\right)}}{F_{\left(z=\frac{h}{2}\right)}} - L(z) \right) \frac{Q_r - Y}{X} + \left(1 - \frac{F(z)}{F_{\left(z=\frac{h}{2}\right)}} \right) q_{sb} + \frac{F(z)}{F_{\left(z=\frac{h}{2}\right)}} q_{st} \right]^2 dz\, dr \tag{31}$$

$$\Pi'_s = \frac{1}{2}\int_a^b \int_{-h/2}^{h/2} \frac{\tau'^2_{rz}}{\kappa G(z)} dz\, dr = \frac{1}{2}\int_a^b \int_{-h/2}^{h/2} \frac{G(z) Q_r^2}{\kappa C^2} dz\, dr \tag{32}$$

Equating the strain energies appeared in Eqs. (31,32), leads to derivation of the shear correction factor:

$$\kappa=\frac{\int_{a}^{b}\int_{-h/2}^{h/2}\frac{G(z)Q_r^2}{C^2}dz\,dr}{\int_{a}^{b}\int_{-h/2}^{h/2}\frac{1}{G(z)}\left[\left(F(z)\frac{L_{\left(z=\frac{h}{2}\right)}}{F_{\left(z=\frac{h}{2}\right)}}-L(z)\right)\frac{Q_r-Y}{X}+\left(1-\frac{F(z)}{F_{\left(z=\frac{h}{2}\right)}}\right)q_{sb}+\frac{F(z)}{F_{\left(z=\frac{h}{2}\right)}}q_{st}\right]^2dz\,dr} \tag{33}$$

For the special cases where no shear tractions are imposed on the top and bottom surfaces, Eq. (33) reduces to the following expression for the shear correction factor:

$$\kappa=\frac{\int_{a}^{b}\int_{-h/2}^{h/2}\frac{G(z)Q_r^2}{C^2}dz\,dr}{\int_{a}^{b}\int_{-h/2}^{h/2}\frac{1}{G(z)}\left[\left(F(z)\frac{L_{\left(z=\frac{h}{2}\right)}}{F_{\left(z=\frac{h}{2}\right)}}-L(z)\right)\frac{Q_r-Y}{X}+\left(1-\frac{F(z)}{F_{\left(z=\frac{h}{2}\right)}}\right)q_{sb}+\frac{F(z)}{F_{\left(z=\frac{h}{2}\right)}}q_{st}\right]^2dz\,dr} \tag{34}$$

If no shear tractions are imposed, the shear correction factor reduces to: $\kappa=5/6$, for the isotropic homogeneous plates.

5 Analytical solution of the governing equations

By using Taylor's series expansion, the governing differential equations and the relevant boundary conditions of the functionally graded plate may be transformed into a set of algebraic equations. Solution of the resulting algebraic system of equations gives the desired solution of the problem.

The functions $u_0(r)$, $w(r)$, and $\psi(r)$ are analytic in a domain *R* and can be represented by power series whose centers are located at $r=r_0$.

$$u_0(r)=\sum_{k=0}^{\infty}(r-r_0)^k U_k,\quad w(r)=\sum_{k=0}^{\infty}(r-r_0)^k W_k,\qquad \psi(r)=\sum_{k=0}^{\infty}(r-r_0)^k \Psi_k \tag{35}$$

In practical applications, these series have to be used as finite series. Therefore, Eq. (35) may be rewritten as

$$u_0(r)=\sum_{k=0}^{N}(r-r_0)^k U_k,\quad w(r)=\sum_{k=0}^{N}(r-r_0)^k W_k,\qquad \psi(r)=\sum_{k=0}^{N}(r-r_0)^k \Psi_k \tag{36}$$

In the present research, the *N* value is so chosen that ignorable changes occur in the results due to further increasing this value. In a free vibration analysis, the mode superposition concept may be used to account for the oscillations of the responses:

$$u_0(r,t)=\sum_{k=0}^{N}U_k(r-r_0)^k e^{i\omega t},\ w(r,t)=\sum_{k=0}^{N}W_k(r-r_0)^k e^{i\omega t},\ \psi_r(r,t)=\sum_{k=0}^{N}\Psi_k(r-r_0)^k e^{i\omega t}, \tag{37}$$

Therefore, the static response is associated with $\omega=0$. In the present research, $r_0=0$ is used as the center for the Taylor's series.

The transformed form of the governing equations of the circular plate may be obtained by substituting Eq. (37) into the governing equation (10). Performing some manipulations on the resulting equations, the transformed form of the governing equations may be obtained as follows:

$$\sum_{i=0}^{N}\Big\{A(i+1)(i+3)U_{i+2}+B(i+1)(i+3)\Psi_{i+2}+\omega^2 I_0 U_i+\omega^2 I_1\Psi_i- T_t\Big[\big(1-b\lambda_2+b^2\lambda_3\big)\delta(i)+\big(\lambda_2-2b\lambda_3\big)\delta(i-1)+\lambda_3\delta(i-2)\Big]- T_b\Big[\big(1-b\gamma_2+b^2\gamma_3\big)\delta(i)+\big(\gamma_2-2b\gamma_3\big)\delta(i-1)+\gamma_3\delta(i-2)\Big]\Big\}r^i=0 \tag{38}$$

$$\sum_{i=0}^{N}\Big\{B(i+1)(i+3)U_{i+2}+D(i+1)(i+3)\Psi_{i+2}-\tilde{A}\big[\Psi_i+(i+1)W_{i+1}\big]+\omega^2 I_1 U_i+\omega^2 I_2\Psi_i-\frac{h}{2}T_t\Big[\big(1-b\lambda_2+b^2\lambda_3\big)\delta(i)+\big(\lambda_2-2b\lambda_3\big)\delta(i-1)+\lambda_3\delta(i-2)\Big]+\frac{h}{2}T_b\Big[\big(1-b\gamma_2+b^2\gamma_3\big)\delta(i)+\big(\gamma_2-2b\gamma_3\big)\delta(i-1)+\gamma_3\delta(i-2)\Big]\Big\}r^i=0 \tag{39}$$

$$\sum_{i=0}^{N}\Big\{\tilde{A}\big[(i+2)\Psi_{i+1}+(i+2)^2W_{i+2}\big]+\omega^2 I_0 W_i-q_0\Big[\big(1-b\alpha_2+b^2\alpha_3\big)\delta(i)+\big(\alpha_2-2b\alpha_3\big)\delta(i-1)+\alpha_3\delta(i-2)\Big]-k_w\Big[\big(1-b\beta_2+b^2\beta_3\big)W_i+\big(\beta_2-2b\beta_3\big)W_{i-1}+\beta_3 W_{i-2}\Big]+k_s(i+2)^2W_{i+2}\Big\}r^i=0 \tag{40}$$

The most common edge conditions of the circular plates may be expressed as follows:

- Clamped edge:

$$u=0,\quad \psi_r=0,\quad w=0, \tag{41}$$

- Simply supported edge:

$$u=0,\quad N_r=0,\quad M_r=0, \tag{42}$$

- Free edge:

$$N_r=0,\quad M_r=0,\quad Q_r+k_s w_{,r}=0, \tag{43}$$

By substituting Eq. (37) into Eqs. (41-43), the transformed forms of the boundary conditions (around $r_0=0$) are obtained:

- Clamped edge:

$$u\big|_{r=b}=\sum_{i=0}^{N}U_i=0\ ,\quad \psi_r\big|_{r=b}=\sum_{i=0}^{N}\Psi_i=0\ ,\quad w\big|_{r=b}=\sum_{i=0}^{N}W_i=0 \tag{44}$$

- Simply supported edge:

$$u\big|_{r=b}=\sum_{i=0}^{N}U_i=0$$
$$M_r\big|_{r=b}=\sum_{i=0}^{N}\Big\{\big[B(i+1)+\bar{B}\big]U_{i+1}+\big[D(i+1)+\bar{D}\big]\Psi_{i+1}\Big\}=0 \tag{45}$$
$$w\big|_{r=b}=\sum_{i=0}^{N}W_i=0$$

- Free edge:

$$N_r\big|_{r=b}=\sum_{i=0}^{N+1}\Big\{\big[A(i+1)+\bar{A}\big]U_{i+1}+\big[B(i+1)+\bar{B}\big]\Psi_{i+1}\Big\}=0$$

$$M_r\big|_{r=b} = \sum_{i=0}^{N+1}\left\{\left[B(i+1)+\bar{B}\right]U_{i+1}+\left[D(i+1)+\bar{D}\right]\Psi_{i+1}\right\}=0$$
$$Q_r + k_s w_{,r}\big|_{r=b} = \sum_{i=0}^{N+1}\left[\tilde{A}\Psi_i+\left(\tilde{A}+k_s\right)(i+1)W_{i+1}\right]=0 \quad (46)$$

Where

$$\begin{Bmatrix}\bar{A}\\ \bar{B}\\ \bar{D}\end{Bmatrix} = \int_{-h/2}^{h/2}\frac{v(z)E(z)}{1-v(z)^2}\begin{Bmatrix}1\\ z\\ z^2\end{Bmatrix}dz \quad (47)$$

Based on Eqs. (44-46), three boundary conditions are available along the outer edge ($r=b$), that may be employed in solution of Eq. (38-40) and consequently, determination of u_0, ψ and w. Moreover, three additional conditions are required that may be extracted from the regularity conditions at the center of the moderately thick circular plate:

$$\begin{aligned} u\big|_{r=0} &= 0 \qquad \rightarrow U_0 = 0\\ \psi_r\big|_{r=0} &= 0 \qquad \rightarrow \Psi_0 = 0\\ w\big|_{r=0} &= 0 \qquad \rightarrow W_1 = 0 \end{aligned} \quad (48)$$

By substituting U_i, W_i, and $\Psi_i\,(2\le i\le N+2)$ from Eqs. (38-40) into Eqs. (44-46) and applying the regularity conditions (48), the final system of equations will have the following form:

$$\begin{aligned} \chi_{11}^{(N)}U_1+\chi_{12}^{(N)}W_0+\chi_{13}^{(N)}\Psi_1 &= F_1\\ \chi_{21}^{(N)}U_1+\chi_{22}^{(N)}W_0+\chi_{23}^{(N)}\Psi_1 &= F_2\\ \chi_{31}^{(N)}U_1+\chi_{32}^{(N)}W_0+\chi_{33}^{(N)}\Psi_1 &= F_3 \end{aligned} \quad (49)$$

For static bending analysis, $\omega^2=0$ and U_1, W_0 and Ψ_1 may be determined by solving the mentioned system of equations. On the other hand, for free vibration analysis of the circular plate, $F_1=F_2=F_3=0$ and existence of a non-trivial solution for the resulting system of equations requires that:

$$\begin{vmatrix}\chi_{11}^{(N)} & \chi_{12}^{(N)} & \chi_{13}^{(N)}\\ \chi_{21}^{(N)} & \chi_{22}^{(N)} & \chi_{23}^{(N)}\\ \chi_{31}^{(N)} & \chi_{32}^{(N)} & \chi_{33}^{(N)}\end{vmatrix}=0 \quad (50)$$

6 Results and discussions

6.1 Verification of the results and evaluation of the resulting enhancements

Since general correction factors that may be used for functionally graded plates have not been proposed so far, especially for the circular plates, results of present section are compared with results of the first-order shear deformation theories that have used Mindlin's correction factors. However, more but different verifications may be found in the next sections. In this regard, aluminium/alumina circular plates with the following material and geometric specifications are considered:

$$E_m = 70GPa,\quad \rho_m = 2700kg/m^3,\quad \nu_m = 0.33,\quad E_c = 380GPa,\quad \rho_c = 3800kg/m^3,$$
$$\nu_c = 0.26,\quad b = 1m,$$

Therefore, results associated with *g=0* correspond to a pure metallic plate. Results are extracted for various thickness ratios ($\widehat{h} = h/b = 0.01, 0.1, 0.2$) to include the very thin, relatively thin, and relatively thick plates. Gupta et al. [25] have considered the same problem but used an exponential law for variations of the material properties and employed $\kappa = \pi^2/12$ Mindlin's correction factor that is suitable for a plate with infinite extent. Hosseini Hashemi et al. [26] have used the traditional $\kappa = 5/6$ Mindlin shear correction factor. Both references used Mindlin first-order shear-deformation plate theory. For this reason, present results for the first two natural frequencies of the plate are compared with the results correspond to *g=0* of Gupta et al. [25] and *g=1* of Hosseini Hashemi et al. [26] in Table (1). As reference [25], results of Table (1) are extracted for the simply supported, clamped, and free edge conditions. As may be expected, the natural frequencies increase with increasing the volume fraction index. The results are in a good agreement. The maximum discrepancies have occurred between present results and results of reference [26], for the simply supported plates. However, the maximum relative difference is less than 4%. Indeed, the mentioned discrepancies are deviations of results of reference [26] with respect to present results and results of reference [25].

Table 1 A comparison among the first two natural frequencies of the plate, for various thickness ratios, volume fraction indices, and edge conditions.

Edge condition	$\widehat{h} = h/b$		*g=0*		*g=1*		*g=2*	*g=5*	*g=10*	*g=100*
			Present	Ref. [25]	Present	Ref. [26]				
Clamped	0.01	ω_1	25.045	---	37.552	37.552	40.003	43.203	48.677	48.677
		ω_2	97.439	---	146.11	146.11	155.65	168.10	189.38	189.38
	0.1	ω_1	243.85	243.81	366.88	366.91	391.34	422.49	474.13	474.13
		ω_2	895.37	894.53	1355.4	1355.7	1449.7	1564.2	1742.2	1742.2
	0.2	ω_1	453.67	453.21	688.45	688.62	736.78	794.65	882.93	882.93
		ω_2	1485.2	1481.7	2287.1	2288.4	2463.6	2653.3	2895.5	2895.5
Simply supported	0.01	ω_1	12.101	---	19.373	18.144	20.237	21.229	23.521	23.521
		ω_2	72.843	---	110.23	109.22	117.08	125.94	141.58	141.58
	0.1	ω_1	120.02	120.03	192.19	180.08	200.88	210.76	233.31	233.31
		ω_2	692.87	692.52	1052.3	1044.0	1120.9	1205.9	1347.5	1347.5
	0.2	ω_1	234.37	234.29	375.55	352.38	393.17	412.73	455.73	455.73
		ω_2	1227.7	1225.9	1878.7	1869.0	2012.9	2166.5	2390.7	2390.7
Free	0.01	ω_1	22.075	---	33.097	---	35.257	38.078	39.978	42.904
		ω_2	94.209	---	141.25	---	150.48	162.52	170.62	183.10
	0.1	ω_1	217.49	217.47	326.25	---	347.81	375.72	394.31	422.77
		ω_2	884.28	883.83	1331.5	---	1422.9	1537.0	1610.2	1719.9
	0.2	ω_1	417.28	417.11	626.72	---	669.53	723.65	758.71	811.46
		ω_2	1528.1	1525.9	2314.6	---	2490.4	2693.0	2810.6	2976.1

To simultaneously verify the results and evaluate effects of the proposed shear correction factor on enhancing the static results, a titanium-zirconica FGM circular plate with the

following specifications, subjected to a uniformly distributed transverse load is considered as Reddy et al. [27] and Saidi et al. [28]:

$$q_0 = 40N/m^2, E_m/E_c = 0.396, \quad \nu = 0.288, \quad b = 1m,$$

In this case, *g=0* denotes a pure ceramic plate. References [27] and [28] have used a FSDT with a $\kappa = 5/6$ correction factor and a third-order shear-deformation theory (TSDT), respectively. Present results for the dimensionless maximum lateral deflection of the plate ($\bar{w} = 64D_c w/\left(q_0 b^4\right)$) are compared with results of references [27] and [28] in Table (2), for various thickness ratios, volume fraction indices, and simply supported and clamped edge conditions. As may be noted from results appeared in Table (2), present results are closer to results of the third-order shear-deformation theory. It is important to remind that since the order of the transverse shear stress is much lower than that of the bending stresses, the relevant effects on the results are ignorable. Therefore, even ignorable differences in the results may reflect high effects of the proposed shear correction factors. In Figure (2), 3D plots are presented for the transverse and radial distributions of the lateral deflection of plates with clamped and simply supported edge conditions (*q_0=100kPa*, *g=1*, and $\hat{h} = 0.2$), for a better visualization.

Table 2 A comparison among the maximum non-dimensional deflections $\bar{w} = 64D_c w/\left(q_0 b^4\right)$ of FG circular plates under uniform transverse pressures.

Edge condition	*g*	Source	Thickness radius ratio ($\hat{h}$)			
			0.05	0.1	0.15	0.2
Clamped	0	FSDT [27]	2.554	2.639	2.781	2.979
		TSDT [28]	2.553	2.638	2.779	2.975
		Present	2.554	2.638	2.781	2.979
	2	FSDT [27]	1.402	1.444	1.515	1.613
		TSDT [28]	1.402	1.443	1.511	1.606
		Present	1.402	1.443	1.512	1.608
	6	FSDT [27]	1.220	1.257	1.318	1.404
		TSDT [28]	1.220	1.255	1.314	1.397
		Present	1.220	1.255	1.315	1.398
	10	FSDT [27]	1.155	1.190	1.250	1.333
		TSDT [28]	1.154	1.189	1.247	1.327
		Present	1.154	1.189	1.248	1.329
	100	FSDT [27]	1.029	1.063	1.119	1.199
		TSDT [28]	1.029	1.063	1.119	1.197
		Present	1.029	1.063	1.119	1.198
Simply supported	0	FSDT [27]	10.396	10.481	10.623	10.822
		TSDT [28]	10.394	10.479	10.621	10.820
		Present	10.396	10.481	10.623	10.821
	2	FSDT [27]	5.497	5.539	5.610	5.708
		TSDT [28]	5.497	5.538	5.607	5.703
		Present	5.497	5.538	5.607	5.703
	6	FSDT [27]	4.909	4.946	5.007	5.094
		TSDT [28]	4.909	4.944	5.004	5.087
		Present	4.909	4.945	5.004	5.088
	10	FSDT [27]	4.677	4.712	4.772	4.855
		TSDT [28]	4.676	4.711	4.769	4.851
		Present	4.676	4.711	4.770	4.851
	100	FSDT [27]	4.189	4.223	4.280	4.359
		TSDT [28]	4.189	4.223	4.279	4.358
		Present	4.189	4.223	4.279	4.359

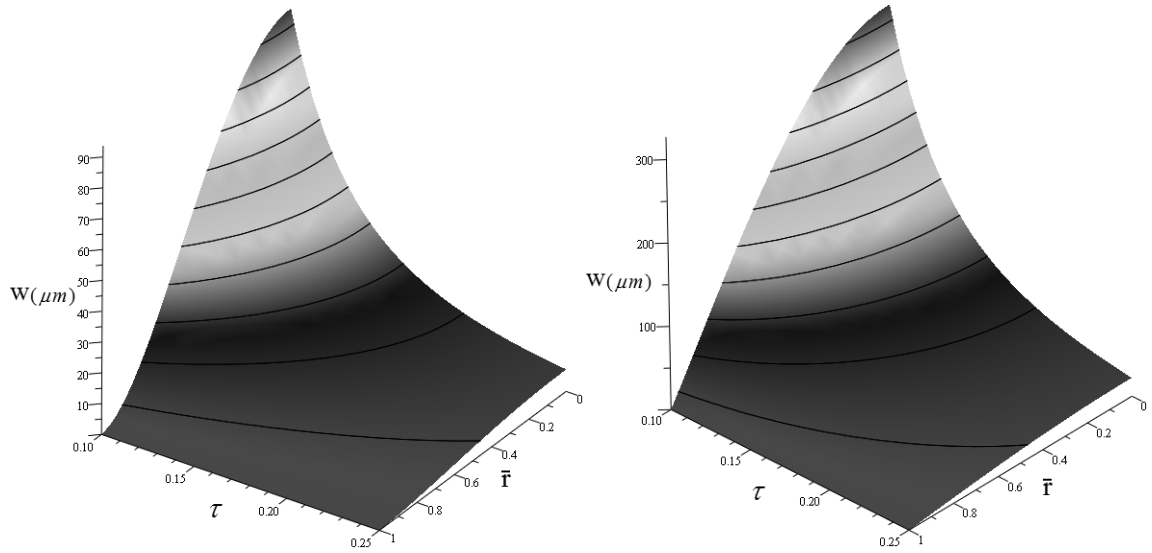

(a) (b)

Figure 2 Through-thickness distribution of the lateral deflection of a: (a) clamped and (b) simply supported FGM plate subjected uniform normal load (q_0*=100kPa*, *g=1*, and $\bar{h} = 0.2$).

6.2 Influence of the shear correction factor on the trough-thickness distribution of the transverse shear stress

To ensure that the proposed shear correction factor and the elasticity-based modifications employed to determine the transverse shear stress have enhanced the results, distribution of the transverse shear stress is plotted for the mid-section (*r=b/2*) of the mentioned titanium-zirconica FGM circular plate. This distribution is compared with those obtained based on the third-order shear-deformation [29] and elasticity [30] theories in Figure (3), for *g=0.5* and *2*.

In Figure (3), the dimensionless transverse shear stress ($\bar{\tau}_{rz} = \tau_{rz} / q$) is plotted versus the dimensionless transverse coordinate ($\bar{z} = z / h$). Although the constitutive-equation-based distribution of the transverse shear stress according to the first-order shear-deformation theories is a uniform and constant one (and therefore, an erroneous one), present distribution is both non-uniform and non-linear, due to using the elasticity correction. Furthermore, while results of the third-order shear-deformation theory exhibit some deviations, results of the present first-order approach with elasticity-based correction are almost coincident with the elasticity results. This comparison confirms that determining the transverse stresses based on the equilibrium requirements leads to more accurate results in comparison to the constitutive-equations-based approach.

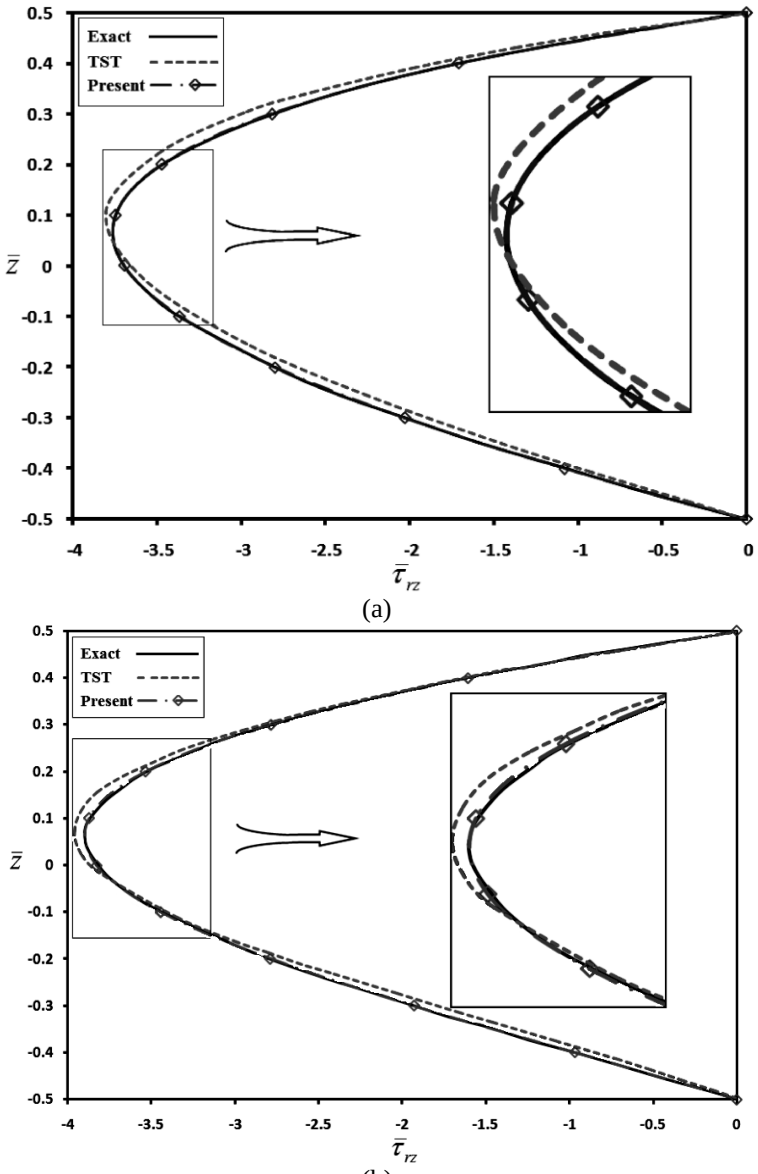

Figure 3 A comparison among the through-thickness distributions of the dimensionless transverse shear stress of a simply supported FGM plate subjected to a uniform transverse pressure, predicted by the present approach and the third-order shear-deformation (TST) [29] and elasticity (exact) [30] theories ($\bar{\tau}_{rz} = \tau_{rz} / q$, $\bar{z} = z / h, r = 0.5b, \hat{h} = h / b$): (a) *g=0.5* and (b) *g=2*.

6.3 Effects of the non-uniformity of the elastic foundation and the applied tractions

The first two natural frequencies of aluminium/alumina plates with linear variations of the material properties (*g=1*) and uniform Winkler elastic foundations are reported in Table (3), for various edge conditions and thickness ratios and compared with those of the three-dimensional elasticity theory. The elasticity results are extracted form ABAQUS software, using the 3D quadratic eight-node axisymmetric elements (CAX8R). As expected, since the elastic foundation increase the stiffness of the structure, the natural frequencies have increased [in comparison with results of Table (1)] due to using Winkler-type elastic foundations. Furthermore, effects of the non-uniformity of the Winkler-type and the Pasternak-type elastic

foundations are investigated and the relevant results are given in Table (3). It is evident that the natural frequencies increase further as a Pasternak-type elastic foundation is added.

Table 3 Influence of the elastic foundation on the first two natural frequencies (Hz) of the aluminium/alumina FG circular with various boundary conditions and thickness ratios (*g=1*).

Edge condition	$\widehat{h}$		$k_s=0$				$k_s=10^7$		
			$k_w=10^8$		$k_w=$	$k_w=$	$k_w=10^8$	$k_w=$	$k_w=$
			Present	FEM(3D)	$10^8(1+r)$	$10^8(1+r+r^2)$		$10^8(1+r)$	$10^8(1+r+r^2)$
Clamped	0.1	ω_1	377.0	378.23	380.67	382.27	383.97	387.58	389.15
		ω_2	1357.8	1364.8	1359.1	1359.9	1366.9	1368.2	1369.0
	0.2	ω_1	691.09	693.21	692.1	692.55	692.93	693.94	694.39
		ω_2	2290.2	2317.2	2290.6	2290.8	2292.7	2293.1	2293.34
	0.3	ω_1	946.35	956.59	946.85	947.07	947.21	947.71	947.93
		ω_2	2844.7	2898.4	2845.0	2845.1	2846.0	2846.3	2846.4
Simply supported	0.1	ω_1	209.68	207.65	217.49	221.43	220.13	227.58	231.35
		ω_2	1053.9	1051.8	1055.6	1056.8	1064.8	1066.5	1067.6
	0.2	ω_1	377.12	363.83	379.29	380.42	380.04	382.20	383.32
		ω_2	1878.3	1847.6	1878.7	1879.0	1881.2	1881.7	1882.0
	0.3	ω_1	541.11	522.34	542.11	542.63	542.45	543.45	543.96
		ω_2	2456.8	2331.8	2457.1	2457.2	2458.3	2458.5	2458.7
Free	0.1	ω_1	337.14	337.41	343.67	348.71	355.22	361.37	366.10
		ω_2	1333.3	1336.9	1334.7	1335.7	1348.08	1349.5	1350.4
	0.2	ω_1	628.62	626.92	630.29	631.57	633.35	635.01	636.28
		ω_2	2317.2	2333.9	2317.5	2317.8	2320.9	2321.3	2321.5
	0.3	ω_1	886.92	889.98	887.66	888.23	889.01	889.75	890.32
		ω_2	2787.0	2782.1	2787.1	2787.2	2787.3	2787.4	2787.5

Results of Table (3) reveal that the natural frequencies associated with the free edge condition are smaller than those of the clamped plate and both are smaller than the natural frequencies of plates with simply supported edges and similar other specifications.

Influences of imposing simultaneous normal and shear stresses and their non-uniformities on radial distribution of the lateral deflection of the clamped and simply supported aluminium/alumina FGM plates (*g=1* and $\widehat{h}=0.2$) is investigated in Figure (4). These results show that imposing shear tractions on the top surface of the FGM plate, reduces the lateral deflection of the plate. Generally, the overall effect of these shear tractions resembles effects of a tensile radial tension; so that both lead to lower lateral deflections.

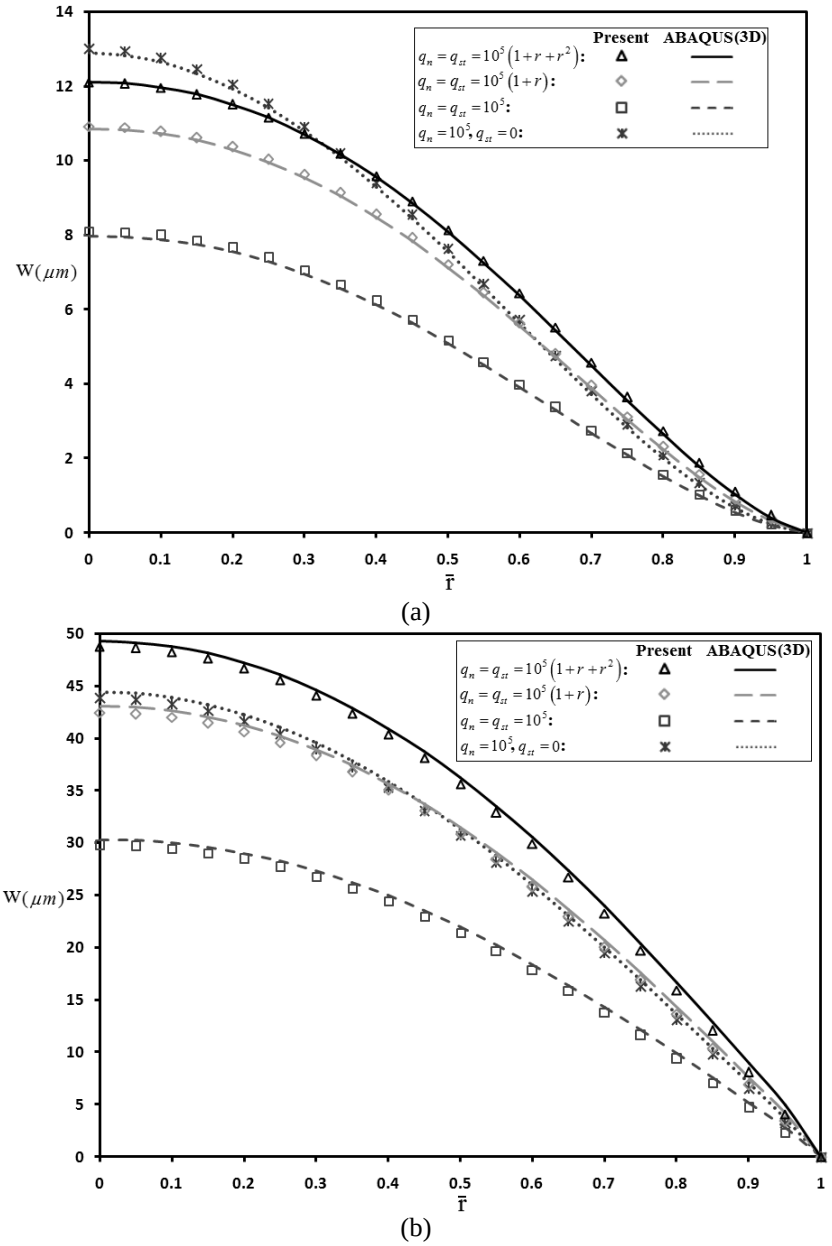

Figure 4 Influences of the normal and shear stresses and their non-uniformities on radial Distribution of the lateral deflection of the: (a) clamped and (b) simply supported aluminium/alumina FGM plates (*g=1*, $\bar{h} = 0.2$).

7 Conclusions

In the present paper, an analytical shear correction factor that is suitable for functionally graded plates (with heterogeneous material properties) that are subjected to non-uniform normal and shear tractions and resting on elastic foundations, is proposed for the first time. This shear correction factor is the most general one, because it considers many issues that have not been treated so far. The shear factor is determined based on equivalence the strain energies of the transverse shear, using elasticity-based corrections. The Taylor transformation technique is employed to analytically solve the governing equations. In contrast to the available first-order formulations, the resulting through-thickness distribution of the shear stress is not uniform; it is bot non-uniform and non-linear. The verification examples have revealed accuracy of the present formulation; so that this accuracy is sometime higher than

that of the third-order shear-deformation theories. Effects of the non-uniform Winkler-Pasternak elastic foundations are discussed in detail. Very rare researches may be found in literature on plates (especially, the circular ones) subjected to shear tractions. Influences of the proposed correction factor are evaluated on results of both the modal and the stress analyses.

References

[1] Reddy, J.N., "Mechanics *of Laminated Composite Plates and Shells: Theory and Analysis*", CRC Press, 2nd Edition, Boca Raton, (2004).

[2] Reddy, J.N., Wang, C.M., and Kitipornchaic, S., "Axisymmetric Bending of Functionally Graded Circular and Annular Plates", European Journal of Mechanics - A/Solids, Vol. 18, pp. 185–199, (1999).

[3] Najafizadeh, M.M., and Eslami, M.R., "First-order-theory-based Thermoelastic Stability of Functionally Graded Material Circular Plates", AIAA Journal, Vol. 40, pp. 1444-1450, (2002).

[4] Najafizadeh, M.M., and Eslami, M.R., "Buckling Analysis of Circular Plates of Functionally Graded Materials under Uniform Radial Compression", International Journal of Mechanical Sciences, Vol. 44, pp. 2479–2493, (2002).

[5] Ma, L.S., and Wang, T.J., "Nonlinear Bending and Post-buckling of a Functionally Graded Circular Plate under Mechanical and Thermal Loadings", International Journal of Solids and Structures, Vol. 40, pp. 3311–3330, (2003).

[6] Whitney, J.M., "Shear Correction Factors for Orthotropic Laminates under Static Load", ASME Journal of Applied Mechanics, Vol. 40, pp. 302-304, (1973).

[7] Mindlin, R.D., "Influence of Rotary Inertia and Shear on Flexural Motions of Isotropic Elastic Plates", Journal of Applied Mechanics, Vol. 18, pp. 31–38, (1951).

[8] Stephen, N.G., "Mindlin Plate Theory: Best Shear Coefficient and Higher Spectra Validity", Journal of Sound and Vibration, Vol. 202, pp. 539-553, (1997).

[9] Andrew, J., "Mindlin Shear Coefficient Determination using Model Comparison", J. Sound Vib. 2006; 294: 125–130.

[10] Liu, Y., and Soh, C.K., "Shear Correction for Mindlin Type Plate and Shell Elements", International Journal for Numerical Methods in Engineering, Vol. 69, pp. 2789–2806, (2007).

[11] Kirakosyan, R.M., "Refined Theory of Orthotropic Plates Subjected to Tangential Force Loads", International Applied Mechanics, Vol. 44, pp. 107–119, (2008).

[12] Batista, M., "Refined Mindlin–Reissner Theory of Forced Vibrations of Shear Deformable Plates", Engineering Structures, Vol. 33, pp. 265–272, (2011).

[13] Huang, N.N., "Influence of Shear Correction Factors in the Higher Order Shear Deformation Lamination Shell Theory", International Journal of Solids and Structures, Vol. 31, pp. 1263-1277, (1994).

[14] Efraim, E., and Eisenberger, M., "Exact Vibration Analysis of Variable Thickness Thick Annular Isotropic and FGM Plates", Journal of Sound and Vibration, Vol. 299, pp. 720–738, (2007).

[15] Nguyen, T.K., Sab, K., and Bonnet, G., "First-order Shear Deformation Plate Models for Functionally Graded Materials", Composite Structures, Vol. 83, pp. 25–36, (2008).

[16] Alipour, M.M., Shariyat, M., and Shaban, M., "A Semi-analytical Solution for Free Vibration of Variable Thickness Two-directional-functionally Graded Plates on Elastic Foundations", International Journal of Mechanics and Materials in Design, Vol. 6, pp. 293-304, (2010).

[17] Shariyat, M., and Alipour, M.M., "A Differential Transform Approach for Modal Analysis of Variable Thickness Two-directional FGM Circular Plates on Elastic Foundations", ISME Journal, Vol. 11, pp. 15-38, (2010).

[18] Shariyat, M., and Alipour, M.M., "Differential Transform Vibration and Modal Stress Analyses of Circular Plates Made of Two-directional Functionally Graded Materials Resting on Elastic Foundations", Archive of Applied Mechanics, Vol. 81, pp. 1289-1306, (2011).

[19] Hetnarski, R.B., and Eslami, M.R., "*Thermal Stresses Advanced Theory and Applications*", Springer Science, New York, (2009).

[20] Shariyat, M., "Non-linear Dynamic Thermo-mechanical Buckling Analysis of the Imperfect Sandwich Plates Based on a Generalized Three-dimensional High-order Global-local Plate Theory", Composite Structures, Vol. 92, pp. 72-85, (2010).

[21] Shariyat, M., "A Generalized High-order Global-local Plate Theory for Nonlinear Bending and Buckling Analyses of Imperfect Sandwich Plates Subjected to Thermo-mechanical Loads", Composite Structures, Vol. 92, pp. 130-143, (2010).

[22] Shariyat, M., "A Nonlinear Double-superposition Global-local Theory for Dynamic Buckling of Imperfect Viscoelastic Composite/Sandwich Plates: A Hierarchical Constitutive Model", Composite Structures, Vol. 93, pp. 1890-1899, (2011).

[23] Shariyat, M., "A Generalized Global-local High-order Theory for Bending and Vibration Analyses of Sandwich Plates Subjected to Thermo-mechanical Loads", International Journal of Mechanical Sciences, Vol. 52, pp. 495-514, (2010).

[24] Shariyat, M., "Non-linear Dynamic Thermo-mechanical Buckling Analysis of the Imperfect Laminated and Sandwich Cylindrical Shells Based on a Global-local Theory Inherently Suitable for Non-linear Analyses", International Journal of Non-Linear Mechanics, Vol. 46, pp. 253-271, (2011).

[25] Gupta, U.S., Lal, R., and Sharma, S., "Vibration of Non-homogeneous Circular Mindlin Plates with Variable Thickness", Journal of Sound and Vibration, Vol. 302, pp. 1–17, (2007).

[26] Hosseini Hashemi, Sh., Fadaee, M., and Es'haghi, M., "A Novel Approach for In-plane, Out-of-plane Frequency Analysis of Functionally Graded Circular/Annular Plates", International Journal of Mechanical Sciences, Vol. 52, pp. 1025–1035, (2010).

[27] Reddy, J.N., Wang, C.M., and Kitipornchai, S., "Axisymmetric Bending of Functionally Graded Circular and Annular Plates", European Journal of Mechanics- A/Solids, Vol. 18, pp. 185–99, (1999).

[28] Saidi, A.R., Rasouli, A., and Sahraee, S., "Axisymmetric Bending and Buckling Analysis of Thick Functionally Graded Circular Plates using Unconstrained Third-order Shear Deformation Plate Theory", Composite Structures, Vol. 89, pp. 110-119, (2009).

Nomenclature

A:	elemental area.
A,B,D:	parameters of the stress resultants.
$\bar{A}, \bar{B}, \bar{D}$:	integrals of the elastic coefficients.
$\tilde{A}$:	parameters of the shear stress.
b:	outer radius of the plate.
C:	constant.
D_c:	bending stiffness of the ceramic.
E:	Young's modulus.
F:	integral of the elastic coefficients; right hand side expression.
g:	is the positive definite power–law index
G:	shear modulus.
h:	thickness.
$\hat{h} = h/b$:	dimensionless thickness.
i:	counter.
$I_0,\ I_1,\ I_2$:	mass density integrals.
k:	Winkler coefficient of the elastic foundation; counter.
k_s:	Pasternak coefficient of the elastic foundation.
k_w:	amplitude of the Winkler coefficient of the elastic foundation.
K:	kinetic energy.
L:	integral of the elastic coefficients.
$M_r,\ M_\theta$:	resultant moments of the radial and circumferential stresses per unit length.
N:	number of the series expressions.
$N_r,\ N_\theta$:	resultant forces of the radial and circumferential stresses per unit length.
P:	representative material property
q_0:	amplitude of the normal traction.
q_n:	normal traction.
$q_{st},\ q_{sb}$:	shear tractions of the top and bottom surfaces.
Q_r:	resultant transverse shear force per unit length.
r:	radial coordinate.
r_0:	center of the series expansion.
t:	time.
T_t, T_b:	amplitudes of the shear tractions of the top and bottom surfaces.
$u,\ u_0$:	radial displacement, radial displacement of the mid-layer.
U:	strain energy.
U_i, W_i:	series coefficients of the in-plane displacement parameters.
V:	energy of the externally applied loads, volume.
V_c, V_m:	volume fractions of the ceramic and metallic materials.
$w,\ w_0$:	transverse displacement, radial displacement of the mid-layer.
$\bar{w}$:	dimensionless lateral deflection.
X, Y:	complicated expressions of the elastic coefficients.
z:	transverse coordinate.
$\bar{z}$:	dimensionless transverse coordinate.

Greek symbols

α_2, α_3: coefficients of the normal traction.
β_2, β_3: coefficients of the Winkler coefficient of the elastic foundation.
χ: elements of the coefficients matrix.
δ: increment; Dirac's delta function.
$\bar{\nabla}$: differentiation operator.
$\varepsilon_r, \varepsilon_\theta, \varepsilon_z$: normal strains in the radial, circumferential, and transverse directions.
$\gamma_2, \gamma_3, \lambda_2, \lambda_3$: coefficients of the shear tractions of the top and bottom surfaces.
γ_{rz}: in-plane shear strain.
κ: shear correction factor.
Γ: boundary of the plate.
ν: Poisson's ratio.
$\prod_s, \prod_s'$: shear strain energies based on the 3D elasticity and FSDT.
θ: circumferential coordinate.
ρ: mass density.
$\sigma_r, \sigma_\theta, \sigma_z$: normal stresses in the radial, circumferential, and transverse directions.
τ_{rz}: in-plane shear stress.
$\bar{\tau}_{rz}$: dimensionless transverse shear stress.
ω: natural frequency.
ψ_r: rotation of the radial section.
Ψ_i: series coefficients of the rotation parameter.

چکیده

ضرایب تصحیح برشی موجود، اساساً برای ورقهای همسانگرد همگن و بر پایه فرض صفر بودن تنشهای برشی موثر بر سطوح بالا و پایین ورق بدست آمده‌اند. در پژوهش کنونی، حالتی کلی‌تری که در آن سطوح رویین و زیرین یک ورق دایره‌ای هدفمند تحت تنشهای قائم و برشی غیر یکنواخت قرار دارند، بررسی شده است. غیریکنواختی توزیع تنشهای قائم و برشی یاد شده ممکن است ناشی از اعمال تنشهای مایل بر سطح رویین ورق و اتکای سطح زیرین ورق بر روی یک تکیه‌گاه الاستیک غیر یکنواخت از نوع ونکلر، باشد. به جای استفاده از روشهای تقریبی عددی، حل معادلات حاکم بر پایه یک روش تحلیلی بدست آمده است. در این راستا، تاثیر ضریب تصحیح برشی تحلیلی پیشنهاد شده بر روی نتایج هر دو نوع تحلیل مودال و تنشی نیز ارزیابی شده است.